Journal of Engineering Mathematics (2024) 147:8
https://doi.org/10.1007/s10665-024-10375-x

Mathematical modeling of breakthrough curves in dynamic column adsorption: analytical solutions and validation

Jimena B. Dima[1,2] · Mariano A. Ferrari[2,3] · Noemi Zaritzky[4]

Received: 4 December 2023 / Accepted: 22 May 2024 / Published online: 27 June 2024

Abstract

Water pollution is a critical global problem. The fixed- bed continuous adsorption column provides the most practical application in the industry for wastewater treatment. The mass transfer process in the column can be described using a mass balance differential equation, and a sorbate–adsorbent interaction rate equation. The objective of this work was to describe the mass transfer in an adsorption column, analyzing the differential equations of the process and their analytical solutions. A general rate equation with four parameters was proposed, adding a zero-order parameter. The general model was solved using Laplace Transform method. The model proposed was applied to describe the adsorption of hexavalent chromium on chitosan biopolymer. The theoretical solution found was satisfactory to estimate the experimental breakthrough curves, and the estimated parameters allowed to predict other curves with different operational conditions. The zero-order parameter added relates to the baseline height of the breakthrough curve. The general model proposed generalizes already known plug flow models based on a single rate equation. The present model uses the information obtained from the column and from the equilibrium batch isotherm, which constitutes a useful tool for describing the dynamic adsorption process and to make decisions on column design.

Keywords Analytical solutions · Column adsorption · Laplace Transform · Rate equation

✉ Mariano A. Ferrari
mferrari7@gmail.com

1 Instituto de BiologÍa de Organismos Marinos, CONICET-CENPAT, Chubut, Argentina

2 Facultad de Ingeniería, Universidad Nacional de la Patagonia S.J.B., Chubut, Argentina

3 Centro para el Estudio de Sistemas Marinos, CONICET-CENPAT, Chubut, Argentina

4 CIDCA and Facultad de Ingeniería, Universidad Nacional de La Plata, Buenos Aires, Argentina

1 Introduction

The contamination of water sources due to the increase in toxic pollutants from effluents, generated by different humans activities, is one of the greatest environmental problems facing mankind today [1–3]. Adsorption is a widely used method to treat industrial waste gas and effluents due to its low cost, high efficiency, and easy operation [4, 5]. Based on the operation mode, adsorption can be generally classified into static adsorption (Batch system) and dynamic adsorption (Continue system). Static adsorption occurs in a closed system containing a desired amount of adsorbent contacting with a certain volume of adsorbate solution, while dynamic adsorption usually occurs in an open system where adsorbate solution continuously passes through a column packed with adsorbent [4, 6]. Dynamic adsorption in fixed-bed columns has advantages due to its simple mode of operation, is suitable for large volumes and easy to scale up. The dynamic adsorption process is usually characterized by the so-called breakthrough curves that represent the outlet concentration of pollutant effluent versus time in a fixed-bed column [7, 8]. In a typical breakthrough curve plot, the outlet concentration remains constant near zero (i.e., the baseline of the curve) until the mass transfer zone starts to reach the tower outlet. Then the outlet concentration rises with s-shaped profile until the bed is saturated with solute [9] (Fig. 1). For column adsorption, how to determine the breakthrough curve is a very important issue because it provides the basic information for the design of a column adsorption system [3, 4, 6].

Mathematical modeling and computational simulations have proven to bring an advantage in terms of costs and time, helping to optimize the adsorption process. Mathematical models can be used for the design, scaling, and optimization of adsorption columns; moreover, analytical solutions (when are available) play a key role in the understanding of the dynamic of adsorption columns. Many mathematical models have been developed to understand the adsorption mechanisms and predict the breakthrough curve of a given adsorption system. Empirical models like Bohart–Adams logistic model are widely used in the literature; however, even actually, an equivalent formulation of the logistic model is commonly referenced as Thomas model in the adsorption research literature [3, 10]. This seems to be a misattribution since the actual Thomas model is a very different looking analytic expression [11]. Likewise, several analytical kinetics models like BDTS, Wolborska, Clark, and MMTF models, among others, are used to describe the breakthrough curves [5, 12]. Mathematical models of the transfer process in the adsorption column can be described by using a mass balance differential equation, and a sorbate–adsorbent interaction equation, or system of equations, related to the rate of adsorption and the equilibrium isotherm observed in batch experiments [13, 14]. Complex models of mass transfer process require the simultaneous solution of a set of coupled partial differential equations and analytical solution may not be obtainable in closed form [13]. In this case, the numerical solution based on the finite element method was studied by different authors to describe breakthrough curves [15, 16]. However, these complex models solved numerically require large calculation times, extensive experimentation to determine the parameters, and computational resources [17]. Analytical solutions have been studied for particular models based on a single rate equation: a linear rate equation was studied by Anzelius [18], a quasi-chemical rate equation by Bohart and Adams [19], and a general model with

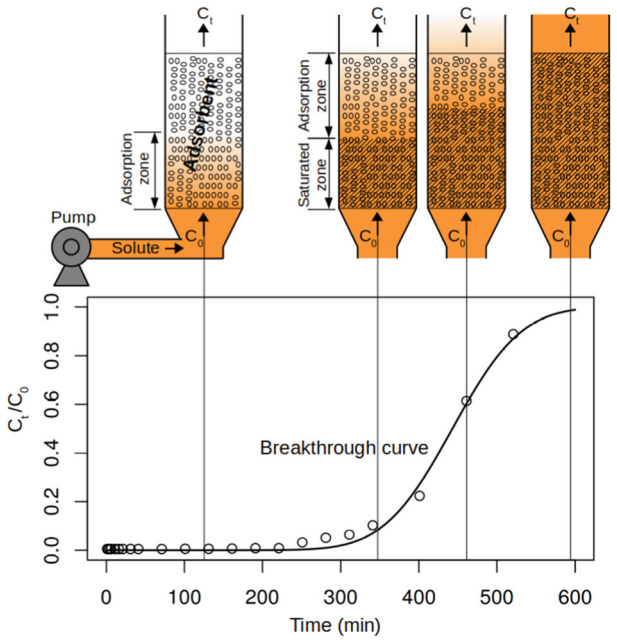

Fig. 1 Scheme of the adsorption process in a continuous system. C_t is the solute concentration at the exit of the column and C_0 is the initial feed concentration. Experimental (points) and modeled (full line) breakthrough curves are described in terms of the relative concentration C_t/C_0 vs. time. The main goal in this work is to develop a general model to predict the breakthrough curve for different operating conditions

a pseudosecond-order rate equation by Thomas [11]. The Thomas model provides a useful description of dynamic adsorption and shows clearly the effect of the isotherm shape on the breakthrough curve [13]. The Thomas model is based on the assumption of Langmuir equilibrium isotherm, one of the most observed in adsorption process [6, 16]. In this sense, Goldstein [20, 21] presented a general solution of the Thomas model that, from our point of view, covers most of the cases studied previously in the literature.

The objective of the present work is to describe the mass transfer process in an adsorption column through the analysis of the differential equations and their analytical solutions. The solution proposed by Goldstein was generalized by adding an independent parameter to the adsorption Langmuir type rate equation, which includes new solutions and allows to describe a variety of breakthrough curves. The model proposed was solved using Laplace Transform method. From the solution obtained, the characteristics of the adsorption curves in relation to the equilibrium isotherms parameters, kinetics parameters, and operational conditions of the column were studied. The theoretical curves obtained were validated with experimental curves of Cr(VI) adsorption on chitosan and reused chitosan particles, at different operating conditions.

2 Adsorption model

When a solute in the liquid phase enters a column packed with a solid adsorbent, the mass transfer process in the column is described by the following differential equation

$$v\frac{\partial c}{\partial z}+\frac{\partial c}{\partial t}+\rho_{\mathrm{r}}\frac{\partial q}{\partial t}-D\frac{\partial^2 c}{\partial z^2}=0, \tag{1}$$

where z (cm) represents the spatial coordinate, given by the height of the column, t (min) is the temporal coordinate, c ($\mathrm{mg\,L^{-1}}$) is the concentration of the solute in the liquid phase, q ($\mathrm{mg\,g^{-1}}$) is the concentration of the solute in the solid adsorbent, v ($\mathrm{cm\,min^{-1}}$) is the interstitial velocity, ρ_{r} ($\mathrm{g\,L^{-1}}$) is the relative density of the adsorbent, and D ($\mathrm{cm^2\,min^{-1}}$) is the axial diffusion coefficient [9]. The term corresponding to axial diffusion will be neglected in what follows considering a plug flow model [13].

The rate of sorbate uptake $\frac{\partial q}{\partial t}$ describes the mass transfer rate of the sorbate from the liquid to the solid phase and is commonly represented by a set of equations comprising the equilibrium constraints to which the mass transfer rate expression must reduce at long times [13]. In simplest models, the rate of the sorption process is expressed as a single rate equation in terms of c and q concentrations.

$$\frac{\partial q}{\partial t}=F(c,q). \tag{2}$$

The form and degree of complexity of the rate equation (2) are responsible for the essential differences among the models proposed in the literature to predict the adsorption breakthrough curves [14, 22, 23]. In the present work, the rate equation of sorbate uptake was represented by Eq. (3) that includes four parameters, adding a zero-order parameter and comprising several cases described in the literature:

$$\frac{\partial q}{\partial t}=kc-k_1q-k_2cq-k_3, \tag{3}$$

where we assume that $k, k_1 \geq 0$ and not both are null. The parameters of this equation are related to the adsorption kinetics and to the equilibrium isotherm, when $\frac{\partial q}{\partial t}=0$:

$$q_{\mathrm{e}}=\frac{kc_{\mathrm{e}}-k_3}{k_1+k_2c_{\mathrm{e}}}. \tag{4}$$

If $k \neq 0$, this formula corresponds to a generalized Langmuir isotherm with a zero-order term and the equilibrium parameters $\hat{k}_j=\frac{k_j}{k}$, for $j=1...3$, can be estimated from batch experiments. Table 1 shows different adsorption models widely used in the literature, and their relationship with the parameters of the general model proposed (3). A linear rate equation was described by Anzelius [18], which is analogous to the equation used to describe heat transfer in a packed bed or double cross-flow heat exchanger. On the other hand, linear rate equations assuming only fluid film driving force or solid film driving force were described by Cooper [24]. A quasi-chemical kinetic rate equation was proposed by Bohart and Adams [19] assuming

Table 1 Different adsorption models widely used in the literature and their relationship with the parameters of the general model proposed

Model	Rate equation	Parameters	General model (3)
Linear rate law	$\frac{\partial q}{\partial t} = k_{\mathrm{L}}(c - b_{\mathrm{L}}q)$	k_{L} ($\mathrm{L\,g^{-1}\,min^{-1}}$) rate coeficient	$k_2 = k_3 = 0$
(Anzelius [18])		b_{L} ($\mathrm{g\,L^{-1}}$) linear isotherm slope	$k = k_{\mathrm{L}}, k_1 = k_{\mathrm{L}}b_{\mathrm{L}}$
Linear rate fluid film diffusion	$\frac{\partial q}{\partial t} = k_{\mathrm{F}}(c - c_{\mathrm{F}})$	k_{F} ($\mathrm{L\,g^{-1}\,min^{-1}}$) rate coeficient	$k_1 = k_2 = 0$
(Cooper [24])		c_{F} ($\mathrm{mg\,L^{-1}}$) equilibrium fluid conc.	$k = k_{\mathrm{F}}, k_3 = k_{\mathrm{F}}c_{\mathrm{F}}$
Linear rate solid film diffusion	$\frac{\partial q}{\partial t} = k_{\mathrm{S}}(q - q_{\mathrm{S}})$	k_{S} ($\mathrm{min^{-1}}$) rate coefficient	$k = k_2 = 0$
(Cooper [24])		q_{S} ($\mathrm{mg\,g^{-1}}$) equilibrium solid conc.	$k_1 = -k_{\mathrm{S}}, k_3 = -k_{\mathrm{S}}q_{\mathrm{S}}$
Quasi chemical kinetic	$\frac{\partial q}{\partial t} = k_{\mathrm{B}}c(q_{\mathrm{B}} - q)$	k_{B} ($\mathrm{L\,mg^{-1}\,min^{-1}}$) rate coefficient	$k_1 = k_3 = 0$
(Bohart–Adams [19])		q_{B} ($\mathrm{mg\,g^{-1}}$) adsorption capacity	$k = k_{\mathrm{B}}q_{\mathrm{B}}, k_2 = k_{\mathrm{B}}$
Pseudosecond-order kinetic	$\frac{\partial q}{\partial t} = k_{\mathrm{T}}c(q_{\mathrm{T}} - q) - b_{\mathrm{T}}q$	k_{T} ($\mathrm{L\,mg^{-1}\,min^{-1}}$), b_{T} ($\mathrm{min^{-1}}$) forward and reverse rate coefficients	$k_3 = 0, k = k_{\mathrm{T}}q_{\mathrm{T}}$
(Thomas [11])		q_{T} ($\mathrm{mg\,g^{-1}}$) adsorption capacity	$k_1 = b_{\mathrm{T}}, k_2 = k_{\mathrm{T}}$

that the adsorption rate is proportional to the concentration of adsorbate. Finally, a pseudosecond-order reversible reaction kinetic equation was described by Thomas [11] assuming a Langmuir equilibrium isotherm (Table 1).

2.1 Normalized equations

Assuming that the liquid solution containing a constant solute concentration (c_0) enters the column; the initials and boundary conditions, for the column initially free of solute, are:

$$\begin{cases} c = c_0, & \text{for } t > 0 \text{ and } z = 0 \\ q = 0, & \text{for } t \geq 0 \text{ and } z \geq vt \end{cases}$$

The saturation concentration of the solute in the adsorbent (q_{sat}) is obtained taking $c = c_0$ and $\frac{\partial q}{\partial t} = 0$ in Eq. (3):

$$q_{\text{sat}} = \frac{kc_0 - k_3}{k_1 + k_2 c_0} \tag{5}$$

Then, considering the normalized concentrations: $u = c/c_0$, $w = q/q_{\text{sat}}$ and applying the following change of variables that rescale the spatial and temporal variables:

$$x = \rho_{\text{r}} \frac{z}{v}, \quad y = \frac{c_0}{q_{\text{sat}}} \left(t - \frac{z}{v} \right) \tag{6}$$

the normalized system was obtained:

$$\begin{aligned} &\frac{\partial u}{\partial x} + \frac{\partial w}{\partial y} = 0 \\ &\frac{\partial w}{\partial y} = ku - aw - buw - d \end{aligned} \tag{7}$$

with boundary conditions:

$$\begin{cases} u(0, y) = 1, & \text{for } y > 0, \\ w(x, 0) = 0, & \text{for } x \geq 0, \end{cases}$$

where

$$a = \frac{q_{\text{sat}}}{c_0} k_1, \quad b = q_{\text{sat}} k_2 \quad \text{and} \quad d = \frac{k_3}{c_0} \tag{8}$$

which satisfy $a + b + d = k$.

2.2 Analytical solution

To solve the system (7), we assume first that $b \neq 0$, solutions for $b = 0$ can be obtained from solutions for $b \neq 0$ as we will see later. Introducing a differential

function $\psi(x, y)$ such that $u = \psi_y$, and $w = -\psi_x$, then the first equation is verified and from the second equation results:

$$-\psi_{xy} = k\psi_y + a\psi_x + b\psi_x\psi_y - d.$$

Further assuming $\psi(0, 0) = 1$, results that $\psi(x, 0) = 1$, for $x \geq 0$, and $\psi(0, y) = 1 + y$, for $y \geq 0$. Now, following Goldstein [20], let us define

$$F(x, y) = \exp\{b[\psi(x, y) + x - y - 1]\},$$

then

$$\begin{aligned} F_x &= Fb(\psi_x + 1) \\ F_y &= Fb(\psi_y - 1) \end{aligned} \tag{9}$$

and

$$\begin{aligned} F_{xy} &= F_x b(\psi_y - 1) + Fb\psi_{xy} \\ &= Fb(\psi_x + 1)b(\psi_y - 1) + Fb(-k\psi_y - a\psi_x - b\psi_x\psi_y + d) \\ &= Fb\left[-\psi_x(b + a) - \psi_y(-b + k) - b + d\right] \\ &= Fb\left[-(a + b)(\psi_x + 1) - (k - b)(\psi_y - 1)\right] \\ &= -(a + b)F_x - (k - b)F_y \end{aligned}$$

since $d = k - a - b$. Then

$$F_{xy} + (k - d)F_x + (k - b)F_y = 0,$$

with

$$\begin{aligned} &F(x, 0) = \exp(bx) \text{ for } x \geq 0, \\ &F(0, y) = 1 \text{ for } y \geq 0. \end{aligned}$$

We applied the Laplace transform over y:

$$\overline{F} = \mathcal{L}(F(x, y), y \to p),$$

then results

$$p\overline{F}_x - F_x(x, 0) + (k - d)\overline{F}_x + (k - b)(p\overline{F} - F(x, 0)) = 0$$

with boundary condition $\overline{F}(0, p) = \frac{1}{p}$, which results an initial value problem over $\overline{F}(x)$

$$(p + k - d)\overline{F}_x + (k - b)p\overline{F} = k\exp(bx), \quad \overline{F}(0) = \frac{1}{p},$$

with solution:

$$\overline{F} = \frac{k}{(k-b)p + (p+k-d)b}\left(\exp(bx) - \exp\Big(\frac{-p(k-b)}{p+k-d}x\Big)\right) + \frac{1}{p}\exp\Big(\frac{-p(k-b)}{p+k-d}x\Big)$$

that we express as

$$\overline{F} = \frac{k}{p+(k-d)b}\exp(bx) - \frac{k}{p+(k-d)b}\exp\Big(\frac{-p(k-b)x}{p+k-d}\Big) + \frac{1}{p}\exp\Big(\frac{-p(k-b)x}{p+k-d}\Big). \tag{10}$$

The inverse transform of the $\overline{F}$ terms can be obtained from known formulas and procedures, see Appendix A, resulting in

$$\begin{aligned} F &= \exp(bx)\exp\Big(-\frac{(k-d)}{k}by\Big) + \exp(bx)\exp\Big(-\frac{(k-d)}{k}by\Big) \\ &\quad \times J\Big(kx, \frac{(k-d)(k-b)}{k}y\Big) + J\Big((k-b)x, (k-d)y\Big) \\ &= \exp(bx)\exp\Big(-\frac{(k-d)}{k}by\Big)\left(1 - J\Big(kx, \frac{(k-d)(k-b)}{k}y\Big)\right) \\ &\quad + J\Big((k-b)x, (k-d)y\Big), \end{aligned} \tag{11}$$

for $k \neq 0$, and

$$F = J\Big((k-b)x, (k-d)y\Big), \tag{12}$$

for $k = 0$. In both cases, the formula for F is valid for $x, y \geq 0$ assuming $k-b, k-d \geq 0$.

The function J is a characteristic of these systems and is defined by

$$J(x, y) = 1 - \mathrm{e}^{-y}\int_0^x \mathrm{e}^{-\tau} I_0(2(\tau y)^{\frac{1}{2}})\mathrm{d}\tau. \tag{13}$$

where I_0 is the modified Bessel function of the first kind, order 0.

Then, to find now the function u, we observed from (9) that

$$u = 1 + \frac{F_y}{bF}. \tag{14}$$

Considering first the case $k \neq 0$ (11), we define

$$N = uF = F + F_y/b,$$

and applying the Laplace transform over y: $\overline{N} = \mathcal{L}(N(x, y), y \to p)$, we have

$$\overline{N} = \overline{F} + \frac{1}{b}\Big(p\overline{F} - F(x, 0)\Big) = \overline{F} + \frac{p}{b}\overline{F} - \frac{1}{b}\exp(bx).$$

Observing that

$$\frac{p}{b}\overline{F} = \frac{k-d}{kp + (k-d)b}\exp\Big(\frac{-p(k-b)x}{p+k-d}\Big) + \frac{p}{(kp + (k-d)b)b}\exp(bx)$$

we have

$$\begin{aligned}\overline{N} = &\frac{d}{kp + (k-d)b}\exp(bx) - \frac{d}{kp + (k-d)b}\exp\Big(\frac{-p(k-b)x}{p+k-d}\Big)\\ &+\frac{1}{p}\exp\Big(\frac{-p(k-b)x}{p+k-d}\Big)\end{aligned} \tag{15}$$

and then, applying the inverse transform

$$\begin{aligned}N = &\frac{d}{k}\exp(bx)\exp\Big(-\frac{(k-d)}{k}by\Big)\Big(1 - J\Big(kx, \frac{(k-d)(k-b)}{k}y\Big)\Big)\\ &+J\Big((k-b)x, (k-d)y\Big).\end{aligned}$$

The solution is then $u(x, y) = \frac{N}{F}$, whenever $x, y, k-b, k-d \geq 0$, and we remark that can be expressed in terms of dimensionless parameters $\hat{b} = \frac{b}{k}$, $\hat{d} = \frac{d}{k}$ with dimensionless variables kx, ky. Indeed, for example, F given in (11) can be expressed as:

$$F = \exp(\tfrac{b}{k}kx)\exp\Big(-(1-\tfrac{d}{k})\tfrac{b}{k}ky\Big)\Big(1 - J\Big(kx, (1-\tfrac{d}{k})(1-\tfrac{b}{k})ky\Big)\Big) + J\Big((1-\tfrac{b}{k})kx, (1-\tfrac{d}{k})ky\Big),$$

and a similar expression can be obtained for N. Thus, since $\frac{a}{k} + \frac{b}{k} + \frac{d}{k} = 1$, the general solution for $k \neq 0$ is

$$u(x, y) = \widehat{u}(kx, ky)$$

where $\widehat{u}(x, y)$ corresponds to the solution for $k = 1$, that is with parameters such that $\hat{a} + \hat{b} + \hat{d} = 1$, and is given by:

$$\widehat{u}(x, y) = \frac{\hat{d}\,A(x, y) + B(x, y)}{A(x, y) + B(x, y)} \tag{16}$$

where

$$\begin{aligned}A(x, y) &= \exp\Big(\hat{b}(x - (1-\hat{d})y)\Big)\Big(1 - J\Big(x, (1-\hat{b})(1-\hat{d})y\Big)\Big)\\ B(x, y) &= J\Big((1-\hat{b})x, (1-\hat{d})y\Big),\end{aligned}$$

with independent parameters $\hat{b}, \hat{d} \in (-\infty, 1]$.

Let us consider now the case $k = 0$ (12), i.e., $a > 0$ and $a + b + d = 0$. In this case, a formula for u can be obtained directly from (14):

$$u(x, y) = 1 - \frac{\mathrm{d}J_y(-bx, -\mathrm{d}y)}{bJ(-bx, -\mathrm{d}y)},$$

for $x, y \geq 0$ assuming $-b, -d \geq 0$. As in the previous case, u can be expressed in terms of dimensionless parameters $\tilde{b} = \frac{b}{a}, \tilde{d} = \frac{d}{a}$ with dimensionless variables ax, ay:

$$u(x, y) = 1 - \frac{\frac{d}{a} J_y\left(-\frac{b}{a}ax, -\frac{d}{a}ay\right)}{\frac{b}{a} J\left(-\frac{b}{a}ax, -\frac{d}{a}ay\right)},$$

and then the general solution for $k = 0$ is:

$$u(x, y) = \widetilde{u}(ax, ay)$$

where $\widetilde{u}(x, y)$ corresponds to the solution for $k = 0$, $a = 1$, $1 + \tilde{b} + \tilde{d} = 0$ and is given by:

$$\widetilde{u}(x, y) = 1 - \frac{(1 + \tilde{b})}{(-\tilde{b})} \frac{J_y(-\tilde{b}x, (1 + \tilde{b})y)}{J(-\tilde{b}x, (1 + \tilde{b})y)}. \tag{17}$$

with independent parameter $\tilde{b} \in [-1, 0]$.

Considering finally the case when $b = 0$, we observe that the system (7) becomes linear and can be solved directly by applying the Laplace Transform method. The solution obtained in this way is

$$u(x, y) = \tfrac{d}{k} + \left(1 - \tfrac{d}{k}\right) J\left(kx, \left(1 - \tfrac{d}{k}\right)ky\right)$$

for $k \neq 0$, and

$$u(x, y) = 1 - ax \exp(-ay)$$

for $k = 0$. Now, considering the standard properties of the function J (see Appendix B), it can be seen that these solutions corresponds to taking the limit $b \to 0$ in the general formulas for $\widehat{u}(x, y)$ and $\widetilde{u}(x, y)$. In fact, taking $\hat{b}, \tilde{b} \to 0$ in (16) and (17), we have:

$$\widehat{u}(x, y) = \hat{d} + (1 - \hat{d}) J(x, (1 - \hat{d})y)$$

and

$$\widetilde{u}(x, y) = 1 - x \exp(-y).$$

2.3 Normalized breakthrough curves

Setting x and varying $y \in (0, \infty)$ in $\widehat{u}(x, y)$ and $\widetilde{u}(x, y)$, normalized breakthrough curves were obtained for the cases $k \neq 0$ and $k = 0$, respectively. Normalized breakthrough curves were analyzed regarding independent parameters and considering the normalized equilibrium isotherms.

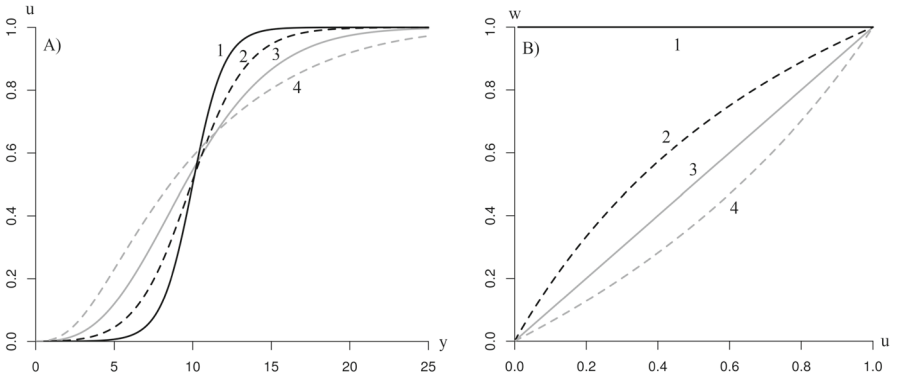

Fig. 2 **A** Normalized breakthrough curves (16) and **B** normalized equilibrium isotherms (18). $x = 10$ and $\hat{d} = 0$ in all cases: (1) $\hat{b} = 1$, Bohart–Adams case, associated to a rectangular isotherm; (2) $\hat{b} = 0.5$, breakthrough curve related to Langmuir isotherm; (3) $\hat{b} = 0$, Anzelius case, associated to a linear isotherm; (4) $\hat{b} = -0.7$, unfavorable case, associated to a convex isotherm

Considering first the case $k \neq 0$, with normalized breakthrough curve $\widehat{u}(x, y)$ (16), there are two independent parameters $\hat{b} = \frac{b}{k}$ and $\hat{d} = \frac{d}{k}$. The corresponding normalized equilibrium isotherm is obtained by setting $\frac{\partial w}{\partial y} = 0$ in (7):

$$w_{\mathrm{e}} = \frac{k u_{\mathrm{e}} - d}{a + b u_{\mathrm{e}}} = \frac{u_{\mathrm{e}} - \hat{d}}{1 - \hat{b} - \hat{d} + \hat{b} u_{\mathrm{e}}}. \tag{18}$$

Figure 2 shows different cases of normalized breakthrough curves related to the normalized equilibrium isotherms. Typical breakthrough curves are s-shaped curves and the slope at the inflection point characterizes the adsorption performance. It can be seen that the slope of the curve depends on the value of $\hat{b}$. The extreme case $\hat{b} = 1$ corresponds to a normalized breakthrough curve associated to a rectangular normalized isotherm $w_{\mathrm{e}} = 1$, which is the most favorable adsorption case. The case $0 < \hat{b} < 1$ corresponds to a normalized breakthrough curve related to Langmuir type adsorption isotherm and $\hat{b} = 0$ represents a normalized breakthrough curve corresponding to a linear isotherm, whereas for $\hat{b} < 0$, an unfavorable adsorption occurs with a convex isotherm.

Figure 3 shows the effect of $\hat{d}$ parameter on normalized breakthrough curves and the corresponding normalized equilibrium isotherms. It is observed that parameter $\hat{d}$ does not change the general profile of the curve but raises or lowers the initial part of the breakthrough curve, where the outlet concentration remains constant (i.e., the baseline) (Fig. 3A). Also, the corresponding normalized adsorption isotherm (Fig. 3B) does not cross the origin and corresponds to an adsorption loss for $\hat{d} > 0$, or gain for $\hat{d} < 0$.

The baseline height of the normalized breakthrough curve can be calculated taking the limit for y tending to 0 in (16). Taking into account that $J(x, 0) = \mathrm{e}^{-x}$, it turns

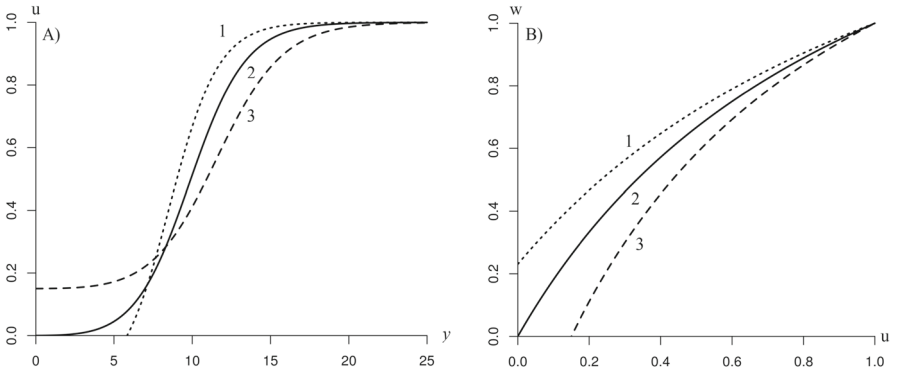

Fig. 3 Effect of parameter $\hat{d}$ on: **A** normalized breakthrough curves (16) and **B** normalized equilibrium isotherms (18). $x = 10$ and $\hat{b} = 0.5$ in all cases: (1) $\hat{d} = -0.15$; (2) $\hat{d} = 0$, (3) $\hat{d} = 0.15$

out that $A(x, 0) = \mathrm{e}^{bx}(1 - \mathrm{e}^{-x})$, $B(x, 0) = \mathrm{e}^{bx}\mathrm{e}^{-x}$ and

$$\widehat{u}(x, 0) = \hat{d} + (1 - \hat{d})\mathrm{e}^{-x}. \tag{19}$$

It can be observed that the baseline height does not depend on the $\hat{b}$ parameter and that it approaches $\hat{d}$ for large x.

Considering now the case $k = 0, a > 0$, with normalized breakthrough curve $\widetilde{u}(x, y)$ (17), there is a single independent parameter $\tilde{b} = \frac{b}{a}$, such that $-1 \leq \tilde{b} \leq 0$. The corresponding normalized equilibrium isotherm is:

$$w_{\mathrm{e}} = \frac{1 + \tilde{b}}{1 + \tilde{b}u_{\mathrm{e}}}. \tag{20}$$

Figure 4 shows different cases of normalized breakthrough curves related to the normalized equilibrium isotherms. It can be seen that the normalized breakthrough curves are concave and the normalized equilibrium isotherms correspond to unfavorable adsorption cases, but with an initial adsorption gain since $\tilde{d} = -(1 + \tilde{b}) \leq 0$. The extreme case $\tilde{b} = 0$ is associated to a rectangular normalized isotherm $w_{\mathrm{e}} = 1$ and corresponds to the solid diffusion model with a linear driving force.

The baseline height of the normalized breakthrough curve, in this case, can be calculated taking the limit for y tending to 0 in (17):

$$\widetilde{u}(x, 0) = 1 - (1 + \tilde{b})x = 1 + \tilde{d}x. \tag{21}$$

2.4 Particular cases of normalized solutions

Particular cases of the equation system (7) were proposed and solved by different authors. These models studied in the past correspond to particular values of $\hat{b}$, $\hat{d}$ and $\tilde{b}$ parameters of the normalized solutions obtained in the present work. Assuming $k \neq 0$

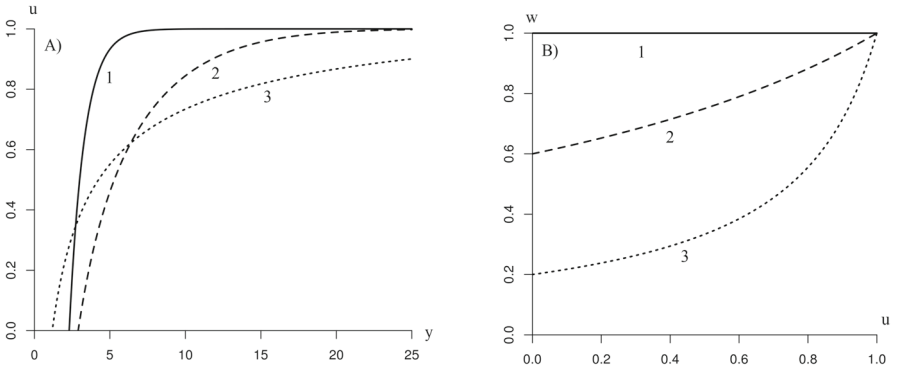

Fig. 4 **A** Normalized breakthrough curves (17) and **B** normalized equilibrium isotherms (20). $x = 10$ in all cases: (1) $\tilde{b} = 0$, solid diffusion with a linear driving force, associated to a rectangular isotherm; (2) $\tilde{b} = -0.4$; (3) $\tilde{b} = -0.8$

and setting $\hat{b} = 1$ in (16), the following solution is obtained:

$$\widehat{u}(x, y) = \frac{\hat{d}(e^x - 1) + e^{(1-\hat{d})y}}{e^x - 1 + e^{(1-\hat{d})y}}.$$

This is the only case where the solution does not depend on function J and coincides with the Bohart–Adams [19] solution when $\hat{d} = 0$ (Fig. 2, case 1). This solution is the most widely used in the literature because it can be approximated with a logistic function [3, 10].

As was previously observed, considering the case $\hat{b} = 0$ in the normalized solution (16) results:

$$\widehat{u}(x, y) = \hat{d} + (1 - \hat{d})J(x, (1 - \hat{d})y).$$

In particular, when $\hat{d} = 0$, this solution coincides with the one described by Anzelius [18] for a heat transfer problem (Fig. 2, case 3), whereas when $\hat{d} = 1$, the solution is constant and correspond to a film diffusion model with a linear driving force, studied by Cooper [24]. The case when $k = 0$ and $\tilde{b} = 0$ (Fig. 4, case 1) also was described in Cooper [24] and corresponds to the solid diffusion model with a linear driving force:

$$\widetilde{u}(x, y) = 1 - x \exp(-y).$$

Finally, the case $k > 0$, $\hat{d} = 0$ and $0 < \hat{b} < 1$ was solved by Thomas [11] and analyzed by Hiester and Vermeulen [25] and Goldstein [20, 21] (Fig. 2, case 2). This model assume a pseudosecond-order reaction rate for the interaction, and it is associated with the Langmuir adsorption isotherm.

The model proposed in the present work generalizes the one proposed by Goldstein [20], adding an independent zero-order term d to Eq. (7). As was shown in (19) and (21), the parameter d relates to the baseline height of the breakthrough curve and represents a constant gain or lose in the adsorption system. The addition of d parameter to the model proposed generalized already known models that includes zero-order terms, like the linear rate film and solid diffusion models [13, 23, 24] (Table 1). A

model that include a zero-order term was also studied by Van Genuchten [26], to describe the chemical transport in solids, assuming a linear rate equation.

In addition, normalized solutions (16) and (17) were obtained using the Laplace Transform, unlike Goldstein, who used an operational method that is very difficult to reference today. The use of Laplace transform also offers the possibility of generalizing the studied system considering other types of boundary conditions or interaction equations.

3 Application to experimental studies

3.1 Experimental work

Experimental work to analyze the adsorption of Cr(VI) in a fixed-bed experimental column using chitosan flakes was carried out to calibrate and validate the proposed model.

Shrimps shells (Pleoticus muelleri) were used for the extraction of chitin and chitosan. The shells were provided by the seafood industries from Puerto Madryn, Patagonia-Argentina. Chitosan particles (CH) were obtained by deacetylation of chitin according to the method proposed by Dima et al. [27].

Experimental adsorption isotherms in batch systems and breakthrough curves were determined using chitosan particles (CH) and also reused chitosan particles (CHR). Reused chitosan particles are CH particles which were utilized in batch adsorption tests and subsequently subjected to desorption in water. CHR adsorption experiments were utilized to validate the applicability of the general model including the zero-order parameter d in the normalized system (7).

Batch studies using CH and CHR were performed according to Dima et al. [27]. Adsorption experiments were carried out by using 80 mg of CH or CHR particles in $50\,mL$ of Cr(VI) solutions of different initial concentrations ranging from 50 to 400 $\mathrm{mg\,L^{-1}}$. All the experiments to investigate the adsorption of Cr(VI) ions onto CH or CHR were carried out in batch tests at pH = 4, under constant stirring.

The fixed-bed column studies with CH and CHR to obtain breakthrough curves were performed according to Dima et al. [3] using a laboratory-scale glass column with an internal diameter of 2 cm and a length of 15 cm. The column was packed with CH or CHR to obtain defined bed heights of the adsorbent (1.5, 2 and 3 cm). Cr(VI) solutions at pH = 4 with different initial concentrations $c_0 = 40\,\mathrm{mg\,L^{-1}}$ for CHR, and 90, $150\,\mathrm{mg\,L^{-1}}$ for CH, were fed continuously at the bottom of the column using a peristaltic pump. Exit chromium solution was collected at regular intervals, until column saturation and Cr(VI) concentrations were determined [3]. For batch and dynamic adsorption experiments, Cr(VI) concentration was measured by 1.5-diphenylcarbazide method, using a UV–visible spectrophotometer operated at 540 nm.

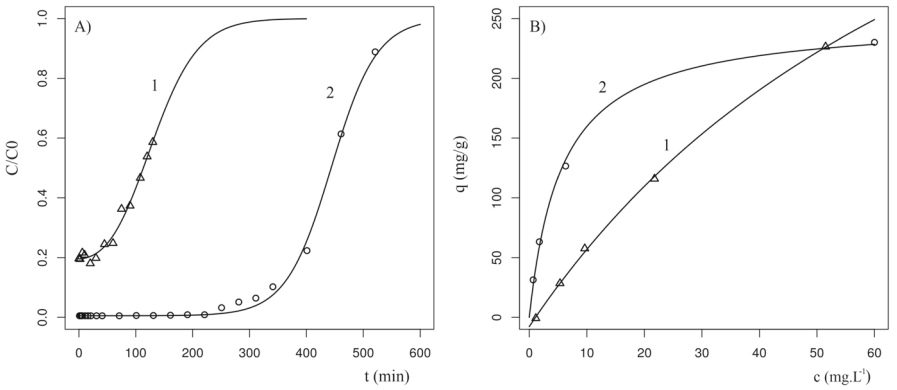

Fig. 5 **A** Breakthrough curves for the adsorption of chromium (VI) in columns filled with (1) chitosan (CH); (2) reused chitosan (CHR), and **B** corresponding batch equilibrium isotherms. Predicted curves (full lines) and experimental data (points)

3.2 Modeling of the adsorption equilibrium isotherms

Equilibrium isotherms of Cr(VI) onto CH and CHR were determined through a nonlinear regression considering Eq. (4) (Fig. 5B). Previous studies [27] and the experimental equilibrium points suggest a Lagmuir type concave isotherm, so only the case $k \neq 0$ was considered. The estimated equilibrium parameters for chitosan (CH) (Fig. 5B, curve 2) resulted: $\hat{k}_1 = 0.023\,\mathrm{g\,L^{-1}}$, $\hat{k}_2 = 0.004\,\mathrm{g\,mg^{-1}}$ and $\hat{k}_3 = 0\,\mathrm{mg\,L^{-1}}$, corresponding to a classical Langmuir isotherm. For reused chitosan (CHR) (Fig. 5B, curve 1) the estimated parameters were: $\hat{k}_1 = 0.141\,\mathrm{g\,L^{-1}}$, $\hat{k}_2 = 0.002\,\mathrm{g\,mg^{-1}}$ and $\hat{k}_3 = 1.083\,\mathrm{mg\,L^{-1}}$. It can be observed that the equilibrium sorption isotherm for CHR is described by a quasi linear isotherm that corresponds to an unfavorable case, due to the decrease of the solid adsorption capacity. Moreover, the zero-order term, $\hat{k}_3 > 0$, of the equilibrium isotherm corresponding to CHR suggests an adsorption loss.

3.3 Estimation of model parameters and validation of the breakthrough curves

Model breakthrough curves of relative concentration were programmed in R [28] and compared, through nonlinear regression, with experimental breakthrough curves. Since $k > 0$ the normalized solution is $u(x, y) = \widehat{u}(kx, ky)$ (16) and taking into account the change of variables (6) the breakthrough curve for a column of height h will be:

$$\frac{c(h,t)}{c_0} = \widehat{u}\left(k\rho_r \frac{h}{v}, k\frac{c_0}{q_{sat}}\left(t - \frac{h}{v}\right)\right) \text{ for } t > \frac{h}{v}. \tag{22}$$

Setting the column design parameters (c_0, h and v), the rest of the parameters were calculated in an iterative procedure as follows:

1. The parameter $\hat{d}$ was set according to (8): $\hat{d} = \frac{\hat{k}_3}{c_0}$.

Table 2 Values of model estimated parameters for CH and CHR

Batch equilibrium parameters					
CH: $\hat{k}_1 = 0.023\ (\mathrm{g\,L^{-1}})$, $\hat{k}_2 = 0.004\ (\mathrm{g\,mg^{-1}})$					
CHR: $\hat{k}_1 = 0.141\ (\mathrm{g\,L^{-1}})$, $\hat{k}_2 = 0.002\ (\mathrm{g\,mg^{-1}})$					
Breakthrough curve parameters Operational conditions	k	ρ_r	$\hat{d}$	$\hat{b}$	RMSE
CH: $c_0 = 90, h = 2, v = 0.95$	0.070	80.300	0.005	0.936	0.014
CHR: $c_0 = 40, h = 2, v = 0.95$	0.251	13.160	0.195	0.252	0.017

c_0 ($\mathrm{mg\,L^{-1}}$), h (cm), v ($\mathrm{cm\,min^{-1}}$), k ($\mathrm{L\,g^{-1}\,min^{-1}}$), ρ_r ($\mathrm{g\,L^{-1}}$)

2. Parameter $\hat{d}$ and the equilibrium parameters $\hat{k}_1$, $\hat{k}_2$ (for each curve) were used to obtain the normalized parameter $\hat{b} = \frac{b}{k}$ according to (8) and (5):

$$\hat{b} = \frac{c_0(1-\hat{d})}{\hat{k}_1 + \hat{k}_2 c_0}\hat{k}_2. \tag{23}$$

3. The kinetic parameter k and the relative density ρ_r were estimated through nonlinear regressions from experimental data (Following an L-BFGS-B algorithm in R [28]).
4. The parameter $\hat{d}$ was recalculated using the baseline height of the experimental breakthrough curves according to (19):

$$\text{Baseline} = \hat{d} + (1-\hat{d})\mathrm{e}^{-x} = \hat{d} + (1-\hat{d})\mathrm{e}^{-\rho_r \frac{h}{v}} \tag{24}$$

5. Steps 2 to 4 were repeated until no differences were found in the recalculated parameters. If $\hat{d}$ was the previously estimated parameter and $\hat{d}^*$ is the recalculated value in step 4, we stop the estimation procedure if $|\hat{d} - \hat{d}^*| < 10^{-5}$ (value that was reached at most in the third iteration).

Table 2 shows all estimated parameters for CH and CHR (k, ρ_r, $\hat{b}$ and $\hat{d}$) and the root-mean square errors ($\mathrm{RMSE} = \sqrt{\sum(c_{\mathrm{exp}} - c_{\mathrm{model}})^2/N}$).

For CH, a column with the following operational conditions was estimated: initial concentration $c_0 = 90\,\mathrm{mg\,L^{-1}}$, height $h = 2\,\mathrm{cm}$ and interstitial velocity $v = 0.95\,\mathrm{cm\,min^{-1}}$ (Fig. 5A, curve 2). The value of $\hat{b}$ obtained is close to 1, which corresponds to a favorable adsorption (Fig. 2A, case 1 rectangular isotherm, Bohart–Adam case). On the other hand, for CHR, a column with the following operational conditions was estimated: $c_0 = 40\,\mathrm{mg\,L^{-1}}$, $h = 2\,\mathrm{cm}$, and $v = 0.95\,\mathrm{cm\,min^{-1}}$ (Fig. 5A, curve 1). In this case, the value of $\hat{b}$ is lower than 1; as $\hat{b}$ approaches zero, the system corresponds to an unfavorable adsorption (Fig. 2A, case 3; Anzelius, linear isotherm case).

The experimental breakthrough curve with CHR was determined to validate the applicability of the general model including the parameter d, when the solid adsorbent in the column changes its adsorption capacity. The experimental breakthrough curve

Table 3 Normalized parameters and errors for predicted CH breakthrough curves considering the batch adsorption experiments and estimated parameters

Operational conditions	$\hat{d}$	$\hat{b}$	RMSE
$c_0 = 90, h = 3, \nu = 0.95$	0.052	0.892	0.116
$c_0 = 90, h = 1.5, \nu = 0.95$	0.006	0.935	0.071
$c_0 = 150, h = 2, \nu = 0.95$	0.033	0.932	0.106

c_0 (mg L^{-1}), h (cm), ν (cm min^{-1})

of the column filled with CH was compared to that of the column containing CHR (reused chitosan) and it can be observed that CHR curve shifts upward due to the lower adsorption capacity of the CHR and the lower retention of chromium in the solid phase. This is reflected in the estimated parameters: for CHR, the values of $\hat{b}$ decreased and the baseline value $\hat{d}$ increased (Table 2, Fig. 5A) which is consistent with its poor adsorption performance since the particle adsorbs less chromium from the liquid stream. The models generally used in the literature to describe breakthrough curves assume a baseline height equal zero. However, the increased in baseline height was observed by different authors for high initial concentration of solute and in different researches of desorption–adsorption cycles in fixed-bed columns [29–32]. The general model proposed in this work incorporates the adsorption loss observed in the CHR through the zero-order parameter d. This parameter allows to describe the initial part of the curve (baseline), achieving an adequate fit of the experimental breakthrough curve.

3.4 Breakthrough curves predictions

New breakthrough curves can be obtained using only the experimental baseline height ($\hat{d}$ parameter), without estimating the parameters k and ρ_r. The same estimated parameters from the CH column described in the previous section (Table 2): $k = 0.07\,\mathrm{L\,g^{-1}\,min^{-1}}$ and $\rho_r = 80.30\,\mathrm{g\,L^{-1}}$ were used to predict other breakthrough curves with different operational conditions, changing initial concentration and column height (Fig. 6). The parameter $\hat{d}$ was calculated using the baseline of the experimental breakthrough curve according to (24) and then normalized parameter $\hat{b}$ was calculated according to (23) for each predicted curve (Table 3). The predicted curves were compared with the experimental data and, in all cases, showed a satisfactory agreement with the experimental breakthrough curves, considering that no parameter was estimated to fit the curves (Fig. 6, Table 3).

The proposed model uses both the data obtained from the column and the equilibrium batch adsorption information to describe the experimental breakthrough curve and can be used to predict other curves with different operating conditions. Starting from a specific adsorbent–adsorbate curve, other curves can be predicted for the same system by changing the operating conditions within certain limits.

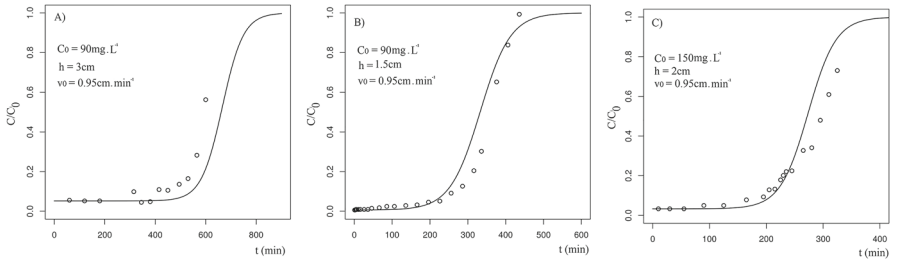

Fig. 6 Predicted and experimental breakthrough curves for the columns filled with CH at different operating conditions. Predicted curves (full line) and experimental curves (points)

4 Conclusion

The mass transfer process in an adsorption column was modeled and described through the analysis of the process differential equations and their analytical solutions. In this work, a general Lagmuir type rate equation with four parameters that covers several cases described in the literature was considered, adding one more parameter to the equations already proposed. The solution found was validated with experimental breakthrough curves. The general solution found was applied to describe the adsorption of the highly toxic transition metal Cr(VI) on the biopolymer chitosan and reused chitosan. The model proposed generalized already known plug flow models based on a single rate equation. The zero-order parameter d relates to the baseline height of the breakthrough curve achieving an adequate fit of the experimental breakthrough curve. The model proposed uses both the data obtained from the column and the information from the equilibrium batch adsorption. The applied method of the Laplace Transform was adequate to solve the problem and also offers the possibility to study more general systems. The theoretical solution found was satisfactory to estimate the CH and CHR breakthrough curves, the estimated parameters for CH allowed to predict other breakthrough curves with different operational conditions, without the need to estimate the parameters. The general model proposed represents an option to describe and predict the adsorption process for wastewater treatment in fixed-bed columns.

Appendix A: Inverse Laplace transforms

In what follows, we sketch how the inverse Laplace transform terms can be obtained.

We observed that all terms of $\overline{F}$ and $\overline{N}$ in (10) and (15) correspond to expressions of the type $C\frac{1}{p-q}\exp\left(\frac{-pz}{p+r}\right)$, for certain C, q, r and z that do not depend of p. We will show that

$$\mathcal{L}^{-1}\left(\frac{1}{p-q}\exp\left(\frac{-pz}{p+r}\right), p \to y\right) = \exp(qy)\ \exp\left(\frac{-qz}{q+r}\right) J\left(\frac{rz}{q+r}, (q+r)y\right), \tag{A1}$$

and from this formula, in fact, results all the inverse transformed terms of F and N.

First, we observed that for $z = 0$, the formula becomes elementary:

$$\mathcal{L}^{-1}\left(\frac{1}{p-q}, p \to y\right) = \exp(qy).$$

Now, for $z \neq 0$, we recall that

$$\mathcal{L}\left(I_0(2z^{\frac{1}{2}}y^{\frac{1}{2}})\right) = \frac{1}{p}\exp\left(\frac{z}{p}\right).$$

If we consider $q = 0$ in (A1) and denoting

$$\frac{1}{p}\exp\left(\frac{-pz}{p+r}\right) = -\int_0^z \frac{1}{p+r}\exp\left(\frac{-p\tau}{p+r}\right)\mathrm{d}\tau + \frac{1}{p}$$

we have, taking into account the definition of J (13),

$$\begin{aligned}
\mathcal{L}^{-1}\left(\frac{1}{p}\exp\left(\frac{-pz}{p+r}\right)\right) &= 1 - \int_0^z \mathcal{L}^{-1}\left(\frac{1}{p+r}\exp\left(\frac{-p\tau}{p+r}\right)\right)\mathrm{d}\tau \\
&= 1 - \mathrm{e}^{-ry}\int_0^z \mathcal{L}^{-1}\left(\frac{1}{p}\exp\left(\frac{-p\tau + r\tau}{p}\right)\right)\mathrm{d}\tau \\
&= 1 - \mathrm{e}^{-ry}\int_0^z \mathrm{e}^{-\tau}\mathcal{L}^{-1}\left(\frac{1}{p}\exp\left(\frac{r\tau}{p}\right)\right)\mathrm{d}\tau \\
&= 1 - \mathrm{e}^{-ry}\int_0^z \mathrm{e}^{-\tau} I_0(2\tau^{\frac{1}{2}}(ry)^{\frac{1}{2}})\,\mathrm{d}\tau = J(z, ry).
\end{aligned}$$

Finally, to show the general case, we observed that

$$\mathcal{L}^{-1}\left(\frac{1}{p-q}\exp\left(\frac{-pz}{p+r}\right)\right) = \exp(qy)\mathcal{L}^{-1}\left(\frac{1}{p}\exp\left(\frac{-pz-qz}{p+q+r}\right)\right).$$

Adding and subtracting $A = \frac{qz}{q+r}$ to the quotient within the last exponential, we obtain

$$\frac{-pz-qz}{p+q+r} = \frac{-p(z-A)}{p+q+r} - A$$

and then

$$\begin{aligned}
\mathcal{L}^{-1}\left(\frac{1}{p}\exp\left(\frac{-pz-qz}{p+q+r}\right)\right) &= \mathrm{e}^{-A}\mathcal{L}^{-1}\left(\frac{1}{p}\exp\left(\frac{-p(z-A)}{p+q+r}\right)\right) \\
&= \mathrm{e}^{-A}J\big((z-A), (q+r)y\big)
\end{aligned}$$

from which the general formula (A1) follows.

Appendix B: *J* function properties

The following properties result directly from the definition (13) and its Laplace transform:

$$
\begin{aligned}
&J(x,0) = \mathrm{e}^{-x}, \quad J(0,y) = 1\\
&\lim_{y\to\infty} J(x,y) = 1, \quad \lim_{x\to\infty} J(x,y) = 0\\
&J(x,y) + J(y,x) = 1 + \mathrm{e}^{-(x+y)} I_0\big(2(xy)^{\frac{1}{2}}\big)\\
&J_x(x,y) = -\mathrm{e}^{-(x+y)} I_0\big(2(xy)^{\frac{1}{2}}\big)\\
&J_y(x,y) = \mathrm{e}^{-(x+y)} \Big(\frac{x}{y}\Big)^{\frac{1}{2}} I_1\big(2(xy)^{\frac{1}{2}}\big)
\end{aligned}
$$

Acknowledgements The authors acknowledge the financial support of Universidad Nacional de La Patagonia, San Juan Bosco (PI 1721/Res. 218-2022), Puerto Madryn, Chubut Argentina. Consejo Nacional de Investigaciones CientÍficas y Tecnológicas (CONICET), and Universidad Nacional de La Plata. The authors also thank Lic. Ivan Mandelman for his collaboration in programming the curves.

Author contributions J.D. and M.F. developed the model and wrote the main manuscript text. J.D. carried out the experimental studies. All authors reviewed the manuscript.

Data availability No datasets were generated or analyzed during the current study.

Declarations

Conflict of interest The authors declare no conflict of interest.

References

1. Bhaumik M, Setshedi K, Maity A, Onyango MS (2013) Chromium (vi) removal from water using fixed bed column of polypyrrole/fe3o4 nanocomposite. Sep Purif Technol 110:11–19
2. Mohan S, Singh DK, Kumar V, Hasan SH (2017) Effective removal of fluoride ions by rgo/zro2 nanocomposite from aqueous solution: fixed bed column adsorption modelling and its adsorption mechanism. J Fluorine Chem 194:40–50
3. Dima JB, Ferrari M, Zaritzky N (2020) Mathematical modeling of fixed-bed columns adsorption: hexavalent chromium onto chitosan flakes. Ind Eng Chem Res 59(34):15378–15386
4. Xu Z, Jg Cai, Bc Pan (2013) Mathematically modeling fixed-bed adsorption in aqueous systems. J Zhejiang Univ, Sci, A 14(3):155–176
5. Juela D, Vera M, Cruzat C, Alvarez X, Vanegas E (2021) Mathematical modeling and numerical simulation of sulfamethoxazole adsorption onto sugarcane bagasse in a fixed-bed column. Chemosphere 280:130687
6. Patel H (2019) Fixed-bed column adsorption study: a comprehensive review. Appl Water Sci 9(3):45
7. Dorado AD, Gamisans X, Valderrama C, Solé M, Lao C (2014) Cr (III) removal from aqueous solutions: a straightforward model approaching of the adsorption in a fixed-bed column. J Environ Sci Health Part A 49(2):179–186
8. Hu Q, Xie Y, Zhang Z (2020) Modification of breakthrough models in a continuous-flow fixed-bed column: mathematical characteristics of breakthrough curves and rate profiles. Sep Purif Technol 238:116399
9. Geankoplis CJ (1997) Transport process and unit operations, 3rd edn. Prentice-Hall, Upper Saddle River
10. Chu KH (2020) Breakthrough curve analysis by simplistic models of fixed bed adsorption: in defense of the century-old Bohart–Adams model. Chem Eng J 380:122513

11. Thomas HC (1944) Heterogeneous ion exchange in a flowing system. J Am Chem Soc 66(10):1664–1666
12. Salim NAA, Fulazzaky MA, Puteh MH, Khamidun MH, Yusoff ARM, Abdullah NH, Fulazzaky M, Zaini MAA (2022) Mass transfer kinetics and mechanisms of phosphate adsorbed on waste mussel shell. Water Air Soil Pollution 233(6):223
13. Ruthven DM (1984) Principles of adsorption and adsorption processes. Wiley, New York
14. Azizian S (2004) Kinetic models of sorption: a theoretical analysis. J Colloid Interface Sci 276(1):47–52
15. Díaz-Blancas V, Aguilar-Madera C, Flores-Cano J, Leyva-Ramos R, Padilla-Ortega E, Ocampo-Pérez R (2020) Evaluation of mass transfer mechanisms involved during the adsorption of metronidazole on granular activated carbon in fixed bed column. J Water Process Eng 36:101303
16. Franco DS, Fagundes JL, Georgin J, Salau NPG, Dotto GL (2020) A mass transfer study considering intraparticle diffusion and axial dispersion for fixed-bed adsorption of crystal violet on pecan pericarp (carya illinoensis). Chem Eng J 397:125423
17. Aguilera P, Ortiz FG (2016) Prediction of fixed-bed breakthrough curves for H2S adsorption from biogas: importance of axial dispersion for design. Chem Eng J 289:93–98
18. Anzelius A (1926) Über erwärmung vermittels durchströmender medien. ZAMM J Appl Math Mech Z Angew Math Mech 6(4):291–294
19. Bohart G, Adams E (1920) Some aspects of the behavior of charcoal with respect to chlorine. J Am Chem Soc 42(3):523–544
20. Goldstein S (1953) On the mathematics of exchange processes in fixed columns. I. Mathematical solutions and asymptotic expansions. Proc R Soc Lond A 219(1137):151–171
21. Goldstein S (1953) On the mathematics of exchange processes in fixed columns. II. The equilibrium theory as the limit of the kinetic theory. Proc R Soc Lond A 219(1137):171–185
22. Chu KH (2010) Fixed bed sorption: setting the record straight on the Bohart-Adams and Thomas models. J Hazard Mater 177(1–3):1006–1012
23. Chatterjee A, Schiewer S (2014) Multi-resistance kinetic models for biosorption of CD by raw and immobilized citrus peels in batch and packed-bed columns. Chem Eng J 244:105–116
24. Cooper RS (1965) Slow particle diffusion in ion exchange columns. Ind Eng Chem Fundam 4(3):308–313
25. Hiester NK, Vermeulen T (1952) Saturation performance of ion exchange and adsorption columns. Chem Eng Prog 48(10):505–516
26. Van Genuchten MT (1981) Analytical solutions for chemical transport with simultaneous adsorption, zero-order production and first-order decay. J Hydrol 49(3–4):213–233
27. Dima JB, Sequeiros C, Zaritzky NE (2015) Hexavalent chromium removal in contaminated water using reticulated chitosan micro/nanoparticles from seafood processing wastes. Chemosphere 141:100–111
28. R Core Team (2023) A language and environment for statistical computing. R Foundation for Statistical Computing, Vienna
29. Vieira M, Esquerdo V, Nobre L, Dotto G, Pinto L (2014) Glass beads coated with chitosan for the food azo dyes adsorption in a fixed bed column. J Ind Eng Chem 20(5):3387–3393
30. Ngah WW, Teong L, Toh R, Hanafiah M (2012) Utilization of chitosan–zeolite composite in the removal of Cu(II) from aqueous solution: adsorption, desorption and fixed bed column studies. Chem Eng J 209:46–53
31. Patino Y, Diaz E, Ordonez S (2016) Pre-concentration of nalidixic acid through adsorption-desorption cycles: adsorbent selection and modeling. Chem Eng J 283:486–494
32. Niasar HS, Das S, Xu CC, Ray MB (2019) Continuous column adsorption of naphthenic acids from synthetic and real oil sands process-affected water (OSPW) using carbon-based adsorbents. Chemosphere 214:511–518